Multi-Objective Dynamic Programming for Saturn Moon Tours Design

Andrea Bellome [(1)], Joan-Pau Sánchez [(1)], Jose Carlos García Mateas[(1)], Arnaud Boutonnet [(2)], Waldemar Martens [(2)], Marcello Sciarra [(3)], David Morante [(3)], Pablo Hermosin [(3)]

[(1)] *ISAE-Supaero*
Toulouse, France
andrea.bellome2@isae-supaero.fr
joan-pau.sanchez@isae-supaero.fr

[(2)] *ESA European Space Operations Centre*
Darmstadt, Germany
Arnaud.Boutonnet@esa.int
Waldemar.Martens@esa.int

[(3)] *Deimos Space*
Madrid, Spain
marcello.sciarra@deimos-space.com
david.morante@deimos-space.com

***Abstract* – This paper introduces a three-step pipeline for the automated design of moon tours within the Saturn system, responding to the challenges posed by their intricate trajectory design problem. The process involves establishing a time-independent transfers' database, incorporating diverse transfer types such as full- and pseudo-resonant transfers, v-infinity leveraging transfers, and body-change transfers. Subsequently, a tree-exploration approach, guided by multi-objective dynamic programming (MODP), constructs moon tours, ensuring Pareto optimality for competing mission objectives like Δv and time of flight. In contrast to existing approaches, MODP proves to be efficient and effective, yielding novel solutions and fronts that dominate current available ones. The presentation of wide Pareto fronts further emphasizes MODP's ability to navigate complex search spaces, providing valuable insights into mission configuration possibilities. Furthermore, the paper addresses the phasing problem between different moons, demonstrating that un-phased Pareto fronts remain structurally unchanged, providing representative solutions for the corresponding phased fronts.**

I. INTRODUCTION

Since the discovery of Enceladus' geysers made by the Cassini spacecraft [1], visiting Saturn moons has motivated numerous studies and missions' designs [2–5]. ESA's Voyage 2050 programme [6] identifies the aim to explore the gas and ice giant systems by means of remote sensing, landing or, even, returning samples back to the Earth. The classic approach for remote sensing characterisation requires a spacecraft to orbit the specific target planet or moon. Given the high energy, and thus high relative velocity, of any spacecraft entering a gas or ice giant system, a long sequence of moon fly-bys will ultimately be necessary to achieve a sufficiently low relative velocity for a final capture to be implemented; either by a small Δv manoeuvre or enabled by a low energy conduit [7].

The trajectory design of such missions is complicated by the fact that the sequence of moons to be visited is not known a priori; rather, it is an integral part of the mission design process. Moreover, the design of Saturn moon tours is different from a tour in Jupiter system, due to the low gravitational constant of the moons (except for Titan), thus leading to tours with tens of gravity assists. This results in a complex mixed-integer non-linear programming (MINLP) problem [8,9]. In such problems, the performance of a specific mission, in terms of, e.g., propellant consumption and/or mission duration, depends both upon the visiting order of the celestial objects, and on sequence of decisions that include manoeuvres, gravity assists, transfer times, or initial tour epoch. Thus, MINLP problems require the solution of a combinatorial problem mixed with optimal control theory. Moreover, finding optimal trajectories that link any sequence of moons is a difficult task on its own, as a variation of even a single fly-by body will correspond to a significantly different trajectory path. In addition, the challenging multi-objective optimization needs to be tackled to appropriately inform the design with the full extent of mission opportunities.

Several techniques have been developed to design long tours in the gas giants' systems. For example, to build transfers between moons, Strange et al. [2] and Campagnola et al. [3,4] introduced the concept of v-infinity leveraging transfers (VILTs) in the linked-conics model to assess the effect of deep space manoeuvres (DSMs) on the spacecraft relative velocity at different moons' encounters. Techniques to design such transfers in multi-body system are also available [5,10,11]. They extend the search space of possible tours, especially in the so-called endgame problem [5]. Landau [12] also presented a method based on primer vector theory [13] for optimal DSM placing on a known sequence of moons.

To build tours with many transfers as above, typically graph-based algorithms are used [14], that add one transfer at a time and employ some pruning criteria or heuristics to prevent the exploration to grow enormously. For example, Strange et al. [2]; Campagnola et al. [3], Campagnola and Russell [4,5], Palma [15] and Takubo et al. [16] all employ tree-graph exploration based on beam search scheme [17] with pruning criteria (even with multi-objective nature [16]) to manage the search space. Usually, such approaches

are not guaranteed to find global optimal solutions, as these algorithms are known to be incomplete [17], plus they might require computational efforts rising sharply with the number of optimization variables (e.g., number of legs, resonant ratios, or infinite velocity bounds), especially in the complex multi-objective optimization.

Thus, the present paper describes a pipeline to transcribe the mixed-integer nature of the trajectory design problem of Saturn moon tours into a discrete graph made by interconnected nodes. Such nodes correspond to fly-bys at Saturn moons, and the connection between them is ensured via either resonant or pseudo-resonant transfers, also considering small deep space manoeuvres at the apses to leverage the spacecraft velocity relative to the moons. The main novelty introduced by this paper is the application of multi-objective dynamic programming (MODP) to explore the graph, guaranteeing Pareto optimality of competing mission objectives with only moderate computational effort, compared to currently available approaches. Moreover, although the mentioned pipeline does not solve the phasing problem between different moons in preliminary design, an analysis is provided to show that this is unlikely to pose a significant challenge, given the short orbital periods of the Saturn moons, going beyond most of the literature on the topic.

The paper is organized as follows: section II describes the problem of designing moon tours in the Saturn system, based on Tisserand graph representation; section III shows how to build moons' tour on an automatic manner using MODP exploration; section IV finally presents numerical results for relevant test cases.

II. MOON TOURS DESIGN

The term tour indicates a mission that needs to pass-by multiple moons to achieve its objective. For the purposes of the present paper, one wants to reach Enceladus making use of fly-by sequences at Saturn major moons, i.e., Titan, Rhea, Dione, Tethys, and Enceladus, and starting from an equatorial orbit crossing Titan at a given relative velocity, or infinite velocity $\vec{v}_\infty$. Parameters used for Saturn moons are summarised in the Appendix.

Planning moon tours corresponds to solving a MINLP, where the quality of a tour, e.g., in terms of overall Δv consumption and/or Time of Flight (ToF), depends both upon the visiting order of the celestial objects, encoded in a vector of integer variables X, and on the sequence of decisions that include manoeuvres/thrust arcs, fly-bys, transfer times, or initial tour epoch, encoded in a vector of continuous-varying variables y.

A typical MINLP problem for moons' tours design can thus be formulated as follows:

$$\begin{aligned} &Minimize: && f_1(X,y),\dots,f_{n_{obj}}(X,y) \\ &Subject\ to: && \begin{cases} g_i(X,y) \le 0\ \forall\ i=1,\dots,n_{cons} \\ X_{lb} \le X \le X_{ub} \\ y_{lb} \le y \le y_{ub} \end{cases} \end{aligned} \quad (1)$$

where: $f_1(X,y),\dots,f_{n_{obj}}(X,y)$ are the objective functions, e.g., overall Δv consumption and/or ToF, with n_{obj} being their cardinality; $g_i(X,y)$ are the constraint functions, e.g., on v_∞ conditions at each moon, with n_{cons} being their cardinality; X_{lb}, X_{ub}, y_{lb} and y_{ub} represent lower and upper bounds for X and y, respectively.

Due to intrinsic complexities of the problem in Eq. (1), planning moons' tours enters the logic of multi-fidelity design [18], where the first level of fidelity usually corresponds to a Tisserand graph exploration [19]. This is a tool which makes uses of energetic consideration to quickly assess the feasibility of different gravity-assist sequences. Tisserand graphs have been firstly introduced via parametrization of the spacecraft orbital elements with respect to infinity velocity v_∞ [20,21]. The underlying assumption is thus that the spacecraft trajectory and fly-by body orbit intersect. In other words, a linked conics dynamical framework (i.e., patched conics together with a zero-radius sphere of influence) is the model ubiquitously present in most of the preliminary mission design studies [19,22].

Assuming circular-coplanar orbits for the moons and planar orbits for the spacecraft, Tisserand graph equations have the following structure:

$$\begin{cases} \dfrac{r_m}{a} = 2 - \dfrac{1}{v_m^2}\left(v_\infty^2 + v_m^2 + 2v_\infty v_m \cos(\alpha)\right) \\ 3 - \left(\dfrac{v_\infty}{v_m}\right)^2 = \dfrac{r_m}{a} + 2\sqrt{\dfrac{a}{r_m}(1-e^2)} \end{cases} \quad (2)$$

where: $\alpha \in [0,180]$ degrees is the so-called pump angle [2], i.e., the angle between the $\vec{v}_\infty$ and the moon velocity vector, positive counter-clockwise; r_m and v_m are the circular radius and velocity of the moon, respectively; a and e are spacecraft semi-major axis and eccentricity, respectively. It is thus possible to plot the spacecraft orbital loci for different values of (v_∞, α) as in Fig. 1. To reproduce Fig. 1 one uses Eq. (2) alongside $r_p = a(1-e)$ and $r_a = a(1+e)$, where r_p and r_a are spacecraft periapsis and apoapsis, respectively.

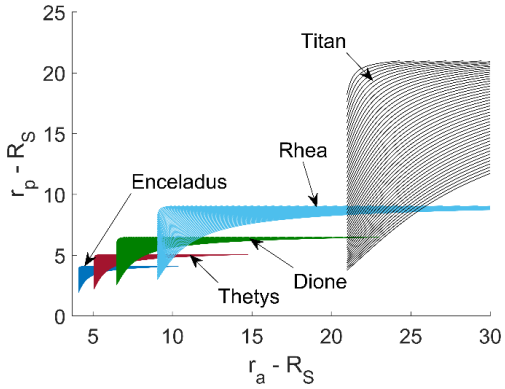

Fig. 1. Tisserand graph for Saturn system. Contours are computed at constant v_∞ with values 0.2, 0.25, 0.3... km/s increasing downwards. The unit of length is the Saturn radius R_S.

From Fig. 1, each line is a set of orbits that cross a given moon at a fixed v_∞ for $\alpha \in [0,180]$ degrees. Thus, a discrete set of infinite velocities at different moons needs to be provided, alongside a step size. The Appendix reports those employed in the present paper. Hence from Eq. (2), the minimum set of design variables needed to describe crossing orbits is (ID, v_∞, α), where ID represents a given moon and its orbital parameters.

An MGA trajectory can thus be seen as a sequence of points (ID, v_∞, α) on the Tisserand graph. To link different points, one has at least three possibilities:

- Resonant or pseudo-resonant transfers. These are transfers on which the spacecraft encounters the same moon consecutively. In full-resonant transfers, the spacecraft and the fly-by body make an integer number of revolutions around the central body, thus the fly-by body is encountered at exactly the same position on its orbit. On such transfers, a ratio of integers exists between the moon and the spacecraft orbit periods. The ratio is expressed as N:M, where N and M are the number of moon and spacecraft revolutions, respectively. A list of N:M ratios used in this paper is presented in the Appendix. In pseudo-resonant transfers, the spacecraft does not encounter the fly-by body at the departure position, but on a different position on its orbit. In terms of design variables, the v_∞ remains the same on such transfers, i.e., no Δv is present, while the pump angle α changes. The ToF on such transfers is derived from the resonant ratio N:M [2]. In pseudo-resonant transfers, for a given v_∞ and resonant ratio N:M, the full-resonant orbit period is slightly increased or decreased until the flight time to the next encounter matches the one of the fly-by body.
- V-infinity Leveraging Transfers (VILTs) [2,3]. In such transfers, a Δv is used to change the spacecraft-moon relative velocity on a pseudo-resonant transfer. The manoeuvres are assumed to occur at one of the apses and parallel to the velocity direction. The Δv depends upon the v_∞ change, and the ToF is derived such that the moon is encountered after the manoeuvre. VILTs are assumed to occur on pseudo-resonant orbits. Details can be found in [2,3]. In terms of design variables, both v_∞ and α change on VILTs due to the presence of the manoeuvre.
- Intersections between different moon contours. These orbits cross two different moons with specified infinity velocities at the same time, and thus represent a possible transfer orbit between two moons. However, these opportunities exist only from an energetic point of view, as no information on the time of flight or moons' phasing is explicitly sought from the Tisserand graphs. Similarly to other works [2,3], one considers $\Delta v = 0$ m/s and $ToF = 0$ days as first approximation, and only successive refinement steps allow to reconstruct the actual trajectory, as shown in section IV.B.

Fig. 2 shows an example of transfers between different points (ID, v_∞, α) on a Tisserand graph. In particular, from an initial orbit crossing Titan, a transfer is performed close to a 4:1 resonance. Then a VILT reduces the v_∞ at the next Titan encounter. A 1:1 resonant transfer is then followed by another Titan fly-by to reduce both r_p and r_a, up until a successive encounter with Rhea. Full details on how to compute resonant transfers, VILTs and intersections are beyond the scope of the present paper, and the interested reader is referred to a vast literature on the topic [2,3].

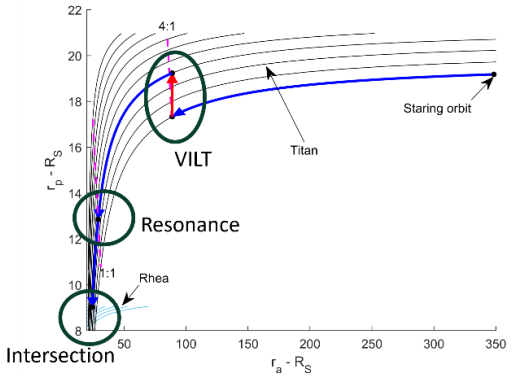

Fig. 2. Representation of different transfers between nodes on Tisserand graph. Blue lines indicate fly-bys, while red line identifies a Δv.

Ultimately, listing all the possible connections between different nodes (ID, v_∞, α) allows to generate database of transfers. Every row of such database is made of $N_s = (ID_s, v_{\infty s}, \alpha_s)$, $N_e = (ID_e, v_{\infty e}, \alpha_e)$, i.e., starting and end node, respectively, and a type of transfer. Such database is then explored using a multi-objective dynamic programming (MODP) approach to find optimal solutions with respect to competing mission objectives, as shown in later section III.

III. EXPLORATION OF THE SEARCH SPACE VIA MULTI-OBJECTIVE DYNAMIC PROGRAMMING

The search space of resonances, VILTs and intersections connecting different orbits (ID, v_∞, α) on Tisserand graphs can be modelled as a *graph* G, defined by two finite sets V and E, such that $G = (V, E)$ [23]. Elements in V are vertices (or nodes) of the graph, i.e., (ID, v_∞, α), while the elements in E are the edges, corresponding to the connection between a pair of vertices, as defined in section II. The graph is *connected* as every element in V can be linked by an element in E, and it is $directed$ as no cycle can be formed (i.e., one vertex can not be visited twice). In this way, one can conveniently model the graph as a $tree$ [24].

Fig. 3 shows an example of a tree-graph for a Tisserand graph exploration. In this case, the nodes encode (ID, v_∞, α), a departure asymptote at a moon, while the edges, represented as arrows in the Figure, encode one of the transfers defined in section II. When expanding the tree-graph, two steps are necessary: 1) expansion, i.e., branching new nodes, 2) selection, i.e., identifying which of the branched nodes need to be further expanded.

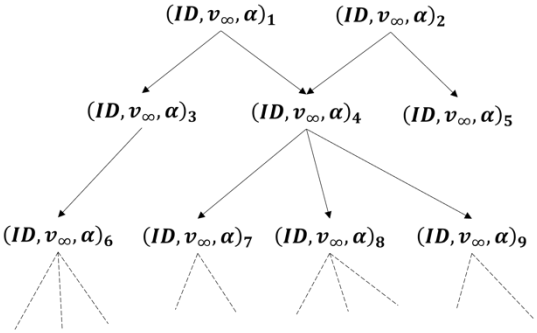

Fig. 3. Tree expansion of nodes representing orbits on Tisserand graphs.

Such appropriate graph transcription, i.e., the identification of the minimum number of variables that are needed to describe a transfer $N_s \rightarrow N_e$, allows the exploitation of the optimal sub-structure property of the fly-by problem [18,19] and, therefore, the application of dynamic programming to the exploration of the search space. Specifically, dynamic programming is used on the selection step of graph exploration, allowing to automatically select nodes that eventually compose the optimal solution. This is possible due to the application of the Bellman's principle of optimality, that is stated here in its multi-objective version [25]:

Regardless of the node at which the spacecraft currently is on the tree-graph, the Pareto-optimal set containing this specific node would include the Pareto-optimal sub-set of nodes before and after the visited one.

This can be seen intuitively from Fig. 4. In particular, from Fig. 4.a, different sequences of nodes (represented as capital letters) arriving to a common node I are mapped in the (f_1, f_2)-plane, where f_1 and f_2 are the objective functions to be minimized as from Eq. (1), e.g., overall ToF and Δv, respectively.

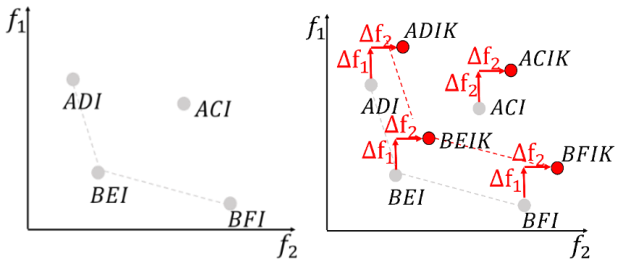

Fig. 4. Representation of different paths arriving to the same node at a specific tree-depth in the (f_1, f_2)-plane (a) and effect of adding a node to the same sequences (b). Dotted lines link nodes on the Pareto front. [19]

A Pareto front of sequences ADI, BEI and BFI is identified, while ACI is the dominated sequence. Since the edges connecting two different nodes do not depend on previously visited nodes, adding another node K implies a variation in all the objectives Δf_1 and Δf_2 and in Fig. 4.b, that is the same for all the sequences. The Pareto front is thus preserved for the sequences ADIK, BEIK and BFIK, and any sequence dominated before adding K is still dominated after the addition of this node, and thus is not needed for further expansion. The resulting is thus an MODP [19] exploration that allows to identify in an automatic manner the optimal Pareto front with the lowest number of paths to be stored in memory.

Algorithm 1. Pseudo-code for MODP exploration.

```
Load the databases, select a starting node (or a pool
P of nodes), a set of user-defined cost functions and
constraints, and a termination criterion
while the termination criterion is not met
    for every node N_i in P
        Find all N_j reachable from N_i
        Save the transfer N_si → N_ej
        Apply the constraints
        Find set U of terminal unique nodes
        for each node in U
            Find all the tours to it
            Evaluate the cost functions
            Identify the Pareto fronts
            Save the tours on the front
            Update P with unique nodes
        end
    end
end
```

Algorithm 1 shows the main steps of the MODP exploration. One needs to select an initial node (or a pool of nodes), some cost functions and constraints. Examples of cost functions are Δv and ToF of the tours, and examples of constraints are provided in later list 1-6. From the databases, one expands the tree of possible nodes reachable from a given starting node $N_i =$

$(ID, v_\infty, \alpha)_i$, by checking the corresponding $(ID, v_\infty)_i = (ID_s, v_{\infty,s})_j$. This implies that a fly-by occurrs at the moon ID_i at the given v_∞. However, such fly-by should be compatible with the constraints, e.g., the altitude should be greater than a given minimum (see also later list 1-6). One then identifies the set of tours that reach unique nodes. For every tour that reaches a unique node, the Pareto front is computed and only the tours on such front are kept for further expansion. This is repeated until a termination criterion is met, e.g., Enceladus is reached with an infinity velocity below a given tolerance.

The set of constraints that are relevant for the present paper are listed below, that follow the rationale of similar literature [2,3,16]. The first 1.-3. are of the operational type and so related with feasibility of the mission, the other 4.-6. are heuristics to manage the search space more efficiently:

1. The first constraint is on the maximum variation on the pump angle α during a fly-by. This is related to the minimum admissible fly-by altitude at each moon, that, for the present report, is 50 km at Rhea, Dione and Tethys, and 1600 km and 25 km at Titan and Enceladus, respectively [16].
2. Maximum Δv between two fly-bys is limited to 50 m/s, while maximum ToF for the whole tour is limited to 1100 days, i.e., approximately 3 years.
3. The tour is composed by different phases, each characterized by fly-bys with the same moon. The last transfer of each phase is an intersection on the Tisserand graph with the next closest moon, and it is used to initialise the phase with the next moon.
4. If going inside the Saturn system, a fly-by can only increase the pump-angle, while a VILT can only decrease the infinity velocity. The opposite occurs if one wants to escape from the Saturn system. This is to avoid cycles in the Tisserand graph exploration, preventing nodes to be visited multiple times.
5. Since many solutions nearly overlap in the Pareto front calculations of MODP, ToF bins are used to reduce the memory load with sensitivity of 5 days. Thus, between two tours arriving to the same node that differ less than 5 days in ToF, only the one with lowest Δv is kept for further expansion. This is similar to the approach in Takubo et al. [16].
6. On a VILT, the Δv manoeuvre is assumed to occur on the first available revolution compatible with the constraints (see also section IV). This is similar to other works [3], where only the mid-revolution is kept.

IV. Results

For the purposes of the present report, moon tours around Saturn are considered, that start at Titan and fly-by main Saturn moons, i.e., Rhea, Dione, Tethys, and Enceladus, although the presented algorithm can also be applied to any planetary system (e.g., Jupiter). Constraints and heuristic criteria employed during the search are already reported in list 1-6 and in the Appendix. Moreover, a simulation is run also considering two more operational constraints. These are: 1) the minimum time between two fly-bys should be greater or equal than 8 days, i.e., $ToF_{fb} \geq 8$ days; 2) the minimum time between a fly-by and a DSM should be greater or equal than 4 days, i.e., $ToF_{DSM} \geq 4$ days. Such values are derived from JUICE mission heritage and simulate flight dynamics constraints for telemetry download and commands upload delays.

Results from the MODP exploration with and without operational constraints are thus presented in following section IV.A. In addition, going beyond most of the current literature, section IV.B presents an approach to solve the phasing problem for some solutions from MODP exploration to assess the Δv and ToF differences introduced by the assumption $\Delta v = 0$ m/s and $ToF = 0$ days on the intersection between contours. The presented pipeline has been implemented in the ESA MIDAS package which is Community Open Source[1].

A. *MODP exploration*

The MODP search is assumed to start from an initial Saturn equatorial orbit crossing Titan, that is $(v_\infty, \alpha) = (1460\frac{m}{s}, 50\ deg)$ similarly to other works in literature [2,3,16]. This corresponds to an orbit with $r_a = 2947611.309$ km and $r_p = 1163229.952$ km. The MODP exploration are stopped when Enceladus is reached with a $v_\infty \leq 250$ m/s. Alongside the cost of VILTs, the overall Δv consumption of a moon tour considers an impulsive manoeuvre to capture the spacecraft around Enceladus with a circular orbit with altitude $h = 100$ km[2].

Results from simulations both with and without operational constraints are represented in Fig. 5. This shows Pareto front solutions as from the MODP approach compared to approaches from literature, i.e., Strange et al. [2], Campagnola et al. [3] and Takubo et al. [16][3]. Each point in the Pareto front represents a different moon tour, in terms of number of fly-bys, moons' encounter conditions, full-resonant transfer, pseudo-resonant transfers and VILTs configurations.

[1] https://midas.io.esa.int/midas/, last accessed March 2024.

[2] Linked-conics approximation is used in this case.

[3] The Pareto front shown from [16] shows only a few representative points hand-picked from a much more populated front. See original plot in [16].

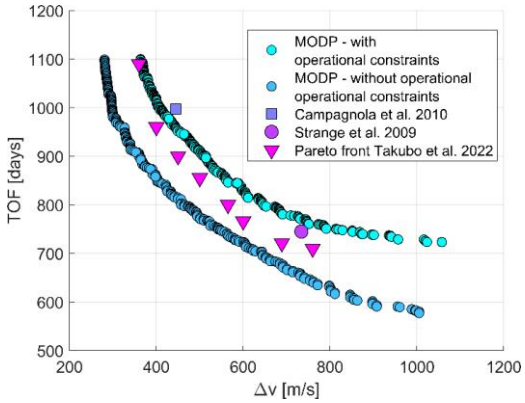

Fig. 5. Pareto fronts from MODP exploration compared to available literature.

As a main result, the Pareto front obtained with MODP exploration without the operational constraints dominates currently available literature, both in quality of solutions and in wideness of the front. This is mainly because the suitable definition of the nodes allows to exploit appropriately the optimal sub-structure property and thus to obtain globally optimal trajectories using MODP. In particular, MODP exploration allows to capture new notable solutions such as tours with minimum overall Δv of approximately 280.6 m/s and mission duration of 1098.78 days to reach Enceladus from the given initial Saturn equatorial orbit crossing Titan. As expected, the Pareto front degrades when operational constraints are included. Such degradation is more pronounced as the ToF decreases, as the MODP exploration is forced to include transfers with higher ToF to be compliant with the constraints. In any case, the minimum Δv solution is only slightly degraded when operational constraints are considered, and the tour showcases an overall consumption of 363.6 m/s with 1099.8 days of time of flight. A summary of each phase of the moons' tours with and without the operational constraints are reported in Table 1. Infinite velocities at the start and at the end of each phase with the given moon are specified in the Table, namely $v_{\infty s}$ and $v_{\infty e}$, as well as the Δv, ToF and number of legs. These solutions correspond to the minimum Δv from the Pareto front of Fig. 5.

Table 1. Summary of minimum Δv solutions. On each phase, the first row is for solution without operational constraints (wo.), while the second row is for solution with constraints (w.). The Δv at Enceladus also considers a 100-km circular orbit insertion. N_L is the number of legs.

Phase		$v_{\infty s}$ [m/s]	$v_{\infty e}$ [m/s]	Δv [m/s]	ToF [days]	N_L
Titan	wo.	1460	1460	0	15.95	2
	w.	1460	1460	0	15.95	2
Rhea	wo.	1700	1350	47.0	420.64	17
	w.	1850	1300	89.7	394.91	15
Dione	wo.	1000	1000	0	167.53	12
	w.	950	900	24.4	195.93	10
Tethys	wo.	800	800	0	215.42	13
	w.	750	700	23.2	240.57	12
Enceladus	wo.	750	200	233.7	279.24	15
	w.	700	200	226.3	252.43	13

Interestingly, all the phases have a lower number of fly-bys with operational constraints, with the only exception of Titan. This is mainly because phases at Rhea, Dione and Tethys with operational constraints employ higher resonant ratios as 3:3, 4:4 and 5:5, respectively, while faster full- and pseudo-resonant 1:1 transfers are sufficient in the case without the constraints. Moreover, phases at Rhea and Enceladus showcase a smaller ToF with the operational constraints, due to the lower number of legs, at the price of higher Δv in the case of Rhea. The phase at Enceladus also has a lower Δv in the case with operational constraints because the start v_∞ is lower than the case without the constraints, while the end v_∞ is the same. In addition, the (slightly) higher Δv with operational constraints can be explained by looking at the v_∞ along the tour. With operational constraints, the initial v_∞ at Rhea is higher than the other case, and then remains lower in the rest of the tour. However, the arrival v_∞ at Enceladus is the same. This suggests that DSMs are in fact needed to compensate the v_∞ penalties in the case with operational constraints.

B. Phasing problem solutions

As from section II, intersections on Tisserand graphs have no explicit information about moons' phasing or transfer time between different moons. Thus, one is interested in assessing the effect of phasing on the overall Δv and ToF of a moon tour resulting from MODP exploration.

In order to do so, an approach based on the authors' previous work is employed [19]. For the MIDAS implementation of the algorithm, the phasing problem is bases on SALTO [26]. Specifically, results from section IV.A are used to fix the set of integer values, i.e., moon encounters and resonant ratios. An MODP optimization is then used to find optimal trajectories between different moons in terms of Δv and ToF, i.e., at the intersections on Tisserand graphs. Without too many details, the trajectories between two different moons are assumed to be Lambert arcs, that are solved over grids of initial tour dates and time of flights. The Δv cost of the given leg is given by the velocity discontinuity occurring at the fly-by epoch between incoming and outgoing $\vec{v}_\infty$, which are solutions of Lambert problem for the given leg. This Δv is shown to well approximate real-world mid-course DSMs, especially when low defects occur, as in the case of Saturn moon tours. Further details are provided in [19].

The start date of the tours is discretized in the whole month of January 2035, with step size of 1 day. Minimum and maximum time of flight for the Lambert problems' solutions are 10 and 45 days for Titan-to-Rhea phase, respectively, and 5 and 25 for all the other phases, respectively. Step sizes are taken as 2% of the orbital

period of the arrival moon. The resulting Δv and ToF of the phased trajectories are shown in Fig. 6. From any point of the un-phased Pareto front, shown in grey in the Figure, a multitude of solutions appear in the phased set. This is because each phased solution differs in terms of initial tour date, time of flight on the Lambert arcs, defects manoeuvres, or VILTs parameters[4].

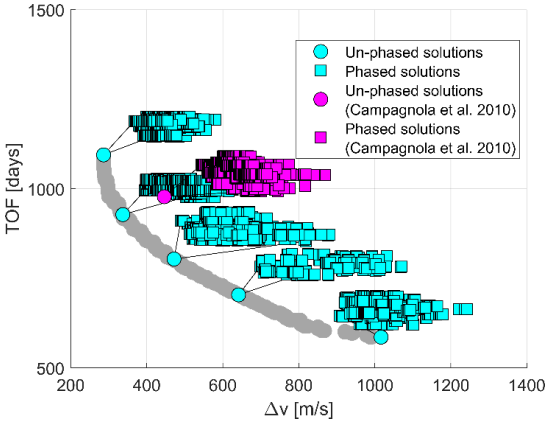

Fig. 6. Un-phased and corresponding phased solutions. The un-phased Pareto front is in grey.

Notably, the phased solutions seem follow a new Pareto front that is scaled up with respect to the un-phased one. This suggests that the phasing problem only moves the points towards the top-right part of the plot, without altering much the un-phased front. Phased solutions towards the bottom-right of the Pareto front experience even a lower Δv with respect to the original un-phased solution, and this is because the VILTs' parameters can vary during the whole tour, allowing some phased solutions to lower the Δv and even performing the Enceladus orbit insertion manoeuvre at lower v_∞. Moreover, solutions that do not belong to the un-phased front are likely not to contribute to the phased one, as shown by the phased solution of the tour from Campagnola et al. [3]. Ultimately, the phasing is unlikely to pose a significant challenge, given the short orbital periods of the Saturn moons.

V. Conclusions

A two-steps pipeline for the automatic design of moon tours within the Saturn system has been presented. This involves the establishment of a time-independent transfers' database, and a subsequent tree-exploration to construct moon tours. By incorporating various transfer types, including full- and pseudo-resonant transfers, v-infinity leveraging transfers, and intersections between infinity velocity contours on Tisserand graph, the pipeline captures the complexity of the mission planning problem. The tree exploration is based on a multi-objective dynamic programming (MODP) scheme that allows to automatically find optimal Pareto fronts of competing mission objectives, namely Δv and time of flight, with respect to different set of constraints.

The experimental results demonstrate the efficiency and effectiveness of the MODP approach over existing literature. Notably, the pipeline yields new and improved solutions, including tours with a remarkable minimum overall Δv of approximately 280 m/s and a mission duration of 1100 days to reach Enceladus from a Saturn equatorial orbit crossing Titan at a given infinite velocity. The presentation of wide Pareto fronts further highlights the MODP's ability to navigate complex search spaces, providing valuable insights into mission configuration possibilities.

Furthermore, the paper addresses the so-called phasing problem at the inter-moon phases. The analysis shows that the structure of the un-phased Pareto front is not significantly altered, and solutions not on the un-phased front are likely not appearing on the corresponding phased front. This suggests that solutions on the un-phased front are representative of those on the corresponding phased front.

VI. Appendix

Table 2 summarises the properties of Saturn moons relevant for this paper, as well as minimum and maximum infinity velocities. Step size for the database generation is 50 m/s. Circular coplanar orbits are assumed. Following

Table 3 shows the list of resonances employed to generate the VILTs databases.

Table 2. Saturn moons' parameters.

	Titan	Rhea	Dione	Tethys	Enceladus
a [km]	1221870	527108	377396	294619	237948
Radius [km]	2574.7	763.8	561.4	531.1	252.1
Period [days]	15.945	4.152	2.737	1.89	1.370
μ [km^3/s^2]	8977.9	153.94	73.110	41.209	7.2094
Min.v_∞ [m/s]	1350	850	750	650	200
Max.v_∞[m/s]	1460	1850	1000	800	800

Table 3. List of resonances for different moons.

Moon	Resonances
Titan	3:1, 2:1, 1:1
Rhea	1:1, 13:7, 9:7, 4:5, 5:3, 3:1, 7:6, 3:2, 7:5, 43, 5:4, 6:5, 15:14, 14:15, 2:2, 3:3, 4:4, 6:7, 2:1, 5:3, 8:5, 7:4, 15:8, 17:8, 9:8, 8:9, 8:7, 7:8, 10:9, 9:10, 11:10, 10:11, 12:11, 11:12, 13:12, 12:13
Dione	1:1, 4:3, 9:7, 5:4, 6:5, 7:6, 8:7, 9:8, 10:9, 11:10, 12:11, 13:12, 19:18, 18:19, 14:15, 12:13, 11:12, 10:11, 9:10, 8:9, 7:8, 6:7, 3:3, 4:4, 5:5, 27:26, 26:27, 26:25, 25:26, 25:24, 24:25
Tethys	1:1, 11:9, 6:5, 7:6, 8:7, 9:8, 10:9, 11:10, 12:11, 13:12, 14:13, 15:14, 19:18, 25:24, 35:34, 34:35, 24:25, 18:19, 14:15, 13:14, 10:11, 9:10, 7:8, 13:15, 4:4, 5:5, 6:6, 34:33, 33:32, 33:32, 32:33, 32:31, 31:32, 31:30, 30:31, 30:29, 29:30, 29:28, 28:29, 28:27, 27:28
Enceladus	1:1, 7:6, 20:17, 15:13, 8:7, 17:15, 9:8, 19:17, 10:9, 21:19, 11:10, 12:11, 13:12, 14:13, 15:14, 16:15, 19:18, 24:23, 17:16, 21:20, 13:11, 22:19, 15:13, 25:22, 18:17

[4] Only the resonant ratios and number of legs are fixed from the un-phased tour.

VII. REFERENCES

[1] J.H. Waite, C.R. Glein, R.S. Perryman, B.D. Teolis, B.A. Magee, G. Miller, J. Grimes, M.E. Perry, K.E. Miller, A. Bouquet, Cassini finds molecular hydrogen in the Enceladus plume: evidence for hydrothermal processes, Science (1979) 356 (2017) 155–159.

[2] N.J. Strange, S. Campagnola, R.P. Russell, Leveraging flybys of low mass moons to enable an Enceladus orbiter, Advances in the Astronautical Sciences 135 (2009) 2207–2225.

[3] S. Campagnola, N.J. Strange, R.P. Russell, A fast tour design method using non-tangent v-infinity leveraging transfer, Celest Mech Dyn Astron 108 (2010) 165–186.

[4] S. Campagnola, R.P. Russell, Endgame problem part 1: V-infinity-leveraging technique and the leveraging graph, Journal of Guidance, Control, and Dynamics 33 (2010) 463–475.

[5] S. Campagnola, R.P. Russell, Endgame problem part 2: multibody technique and the Tisserand-Poincare graph, Journal of Guidance, Control, and Dynamics 33 (2010) 476–486.

[6] F. Favata, G. Hasinger, L.J. Tacconi, C.S. Arridge, K.S. O'Flaherty, Introducing the Voyage 2050 White Papers, contributions from the science community to ESA's long-term plan for the Scientific Programme, Exp Astron (Dordr) 51 (2021) 551–558.

[7] W.S. Koon, J.E. Marsden, S.D. Ross, Constructing a low energy transfer, in: Celestial Mechanics: Dedicated to Donald Saari for His 60th Birthday: Proceedings of an International Conference on Celestial Mechanics, December 15-19, 1999, Northwestern University, Evanston, Illinois, American Mathematical Soc., 2002: p. 129.

[8] M. Schlueter, Nonlinear mixed integer based optimization technique for space applications, (2012).

[9] M. Schlueter, S.O. Erb, M. Gerdts, S. Kemble, J.-J. Rückmann, MIDACO on MINLP space applications, Advances in Space Research 51 (2013) 1116–1131.

[10] R.L. Anderson, S. Campagnola, D. Koh, T.P. McElrath, R.M. Woollands, Endgame design for Europa lander: Ganymede to Europa approach, J Astronaut Sci 68 (2021) 96–119.

[11] D. Canales, K.C. Howell, E. Fantino, Transfer design between neighborhoods of planetary moons in the circular restricted three-body problem: the moon-to-moon analytical transfer method, Celest Mech Dyn Astron 133 (2021) 36.

[12] D. Landau, Efficient maneuver placement for automated trajectory design, Journal of Guidance, Control, and Dynamics 41 (2018) 1531–1541.

[13] D.F. Lawden, Optimal Trajectories for Space Navigation, Butterworths Mathematical Texts, 1963.

[14] A. Majeed, I. Rauf, Graph theory: A comprehensive survey about graph theory applications in computer science and social networks, Inventions 5 (2020) 10.

[15] DFF Palma, Preliminary Trajectory Design of a Mission to Enceladus, Instituto Superior Técnico, 2016.

[16] Y. Takubo, D. Landau, B. Anderson, Automated tour design in the Saturnian system, Celest Mech Dyn Astron 136 (2024) 1–23.

[17] S.C. Shapiro, Encyclopedia of artificial intelligence second edition, John, 1992.

[18] A. Bellome, J.P. Sánchez, J.C.G. Mateas, L. Felicetti, S. Kemble, Modified dynamic programming for asteroids belt exploration, Acta Astronaut 215 (2024) 142–155.

[19] A. Bellome, J.-P. Sánchez, L. Felicetti, S. Kemble, Multiobjective Design of Gravity-Assist Trajectories via Graph Transcription and Dynamic Programming, J Spacecr Rockets (2023) 1–19.

[20] N.J. Strange, J.M. Longuski, Graphical method for gravity-assist trajectory design, J Spacecr Rockets 39 (2002) 9–16.

[21] D. de la Torre Sangrà, E. Fantino, R. Flores, O.C. Lozano, C.G. Estelrich, An automatic tree search algorithm for the Tisserand graph, Alexandria Engineering Journal 60 (2021) 1027–1041.

[22] M. Ceriotti, M. Vasile, MGA trajectory planning with an ACO-inspired algorithm, Acta Astronaut 67 (2010) 1202–1217.

[23] J.M. Harris, Combinatorics and graph theory, Springer, 2008.

[24] D. Jungnickel, D. Jungnickel, Graphs, networks and algorithms, Springer, 2005.

[25] M.M. Kostreva, M.M. Wiecek, Time dependency in multiple objective dynamic programming, J Math Anal Appl 173 (1993) 289.

[26] W. Martens, J. Schoenmaekers, G. Varga, C. Baumgard, O. Ramírez Torralba, P. Muñoz, M. von Looz, R. Mackenzie, SALTO: An Expert-Informed Global Trajectory Design and Optimization Toolkit, in: ESA GNC and ICATT Conference, Sopot, 2023. https://esa-gnc.eu/paper/?paper_id=23004 (accessed March 24, 2024).